Korean J. Chem. Eng., **28**(3), 731-743 (2011)
DOI: 10.1007/s11814-010-0460-8

JOURNAL REVIEW

Nano-structured porous carbon materials for catalysis and energy storage

Dipali Prvine Upare*,, Songhun Yoon*, and Chul Wee Lee*,†**

*Green Chemistry Division, KRICT, Daejeon 305-600, Korea
**School of Science, University of Science and Technology (UST), Daejeon 305-333, Korea
(*Received 9 September 2010 • accepted 25 October 2010*)

Abstract−Porous carbon materials are of interest in many applications because of their high surface area and physicochemical properties. For particular application, the surface of porous carbon material usually needs to be modified or functionalized according to a specific requirement. In this review, methods of synthesis of porous carbon material core shell structure, methods of functionalizing porous carbon material through direct incorporation of heteroatom in carbon synthesis, halogenation, sulfonation, surface oxidation, grafting are examined. The method of characterizing the functionalized carbon material (bulk, surface, internal and external) and its application in the field of catalysis and energy storage (Li-ion batteries, capacitors/supercapacitors), are also subjects of focus.

Key words: Porous Carbon, Core Shell Structure, Template Synthesis, Surface Modification, Energy Storage, Catalysis

INTRODUCTION

Activated carbons are well known as porous solids with a highly developed apparent surface area. Activated carbon is manufactured industrially from various raw materials such as pine wood, bituminous coal and coconut shell. About 190 process patents and various applications of activated carbon were summarized by Yehaskel [1]. A review of these patents shows that a number of processes and a variety of industrial equipment were used for the production of activated carbon. However, rotary kilns are most widely employed for the manufacture of activated carbon. Most of the materials used to prepare active carbon are mineral carbons and lignocelluloses from the biomass, wood and some agricultural wastes [2]. Due to high surface area, porous carbon can be used extensively as a sorbent for separation process, catalytic support, filter, electrode materials for batteries and gas storage. Porous carbon material can be classified into three types, according to their pore diameters as microporous with pore size<2 nm, mesoporous with 2 nm<pore size <50 nm and macroporous with pore size >50 nm. Research regarding the template synthesis of porous carbon material has continued since the pioneering work of Knox's group [3]. In 1982 Knox and his coworkers demonstrated the concept of structuring porous carbon by templating. Since then, much porous carbon material with uniform pore sizes having micropores, mesopores or macropores, respectively, have been synthesized using various inorganic templates. The mesopores are filled with carbon precursor, such as sucrose, phenol, furfuryl alcohol, phenol-formaldehyde, acetonitrile and polypyrole [4-6], followed by carbonization of precursor and removal of inorganic template. Direct synthesis of porous carbon material using soft template (self assembled template) amphiphilic molecules such as block copolymer and surfactants have been widely employed [7]. Carbon particles can be synthesized under hydrothermal conditions using different biomass such as (glucose, maltose, sucrose, starch) and biomass derivates (5-hydroxymethyl-furfural-1-aldehyde (HMF) and furfural) as carbon sources [8].

The application of these porous carbon materials in catalysis, separation, energy storage, requires surface modification. To increase the number of surface functional groups on carbon material, carbon is usually subjected to post treatment including oxidation, polymer coating and grafting. Specific identification of functional groups requires an array of spectroscopic and non-spectroscopic techniques. Later, techniques will be discussed for characterization of carbonaceous samples with emphasis on functional group analysis.

SYNTHESIS

1. Core/Shell Structured Porous Carbon

There has been a great deal of interest in producing core shell composite materials and capsules with modified structural, optical and surface properties. Unger et al. [9] reported the synthesis of submicrometer size solid core/mesoporous shell (SCMS) silica spheres from the simultaneous sol-gel polymerization of tetrahydroxysilane (TEOS) and octadecyltrimethoxysilane (C18TMS) followed by removal of organic group. Yoon et al. [10] synthesized hollow core/mesoporous shell (HCMS) carbon using solid core/mesoporous shell (SCMC) structured silica as a template. The schematic representation for synthesis of HCMC is shown in Fig. 1. The selective deposition of phenol or divinylbenzene as a carbon source into mesopores of SCMS has been done to preserve the spherical structure of template silica. This gives HCMS carbon, which contains uniform hollow cores and mesoporous shell.

Silicate-1 zeolite core/mesoporous silica shell (ZCMS) structures were synthesized from sol-gel reaction of TEOS with C18TMS on the surface of solid pseudo-hexagonal prismatic shaped silicate-1 zeolite particle [11]. The ZCMS particle was used as template to fabricate a carbon replica structure. ZCMS particles are bimodal microspores core and mesoporous shell structure, so the pore replication process took place only through the mesoporous in the shell resulting in producing hollow core/mesoporous carbon (HCMS),

†To whom correspondence should be addressed.
E-mail: chulwee@krict.re.kr

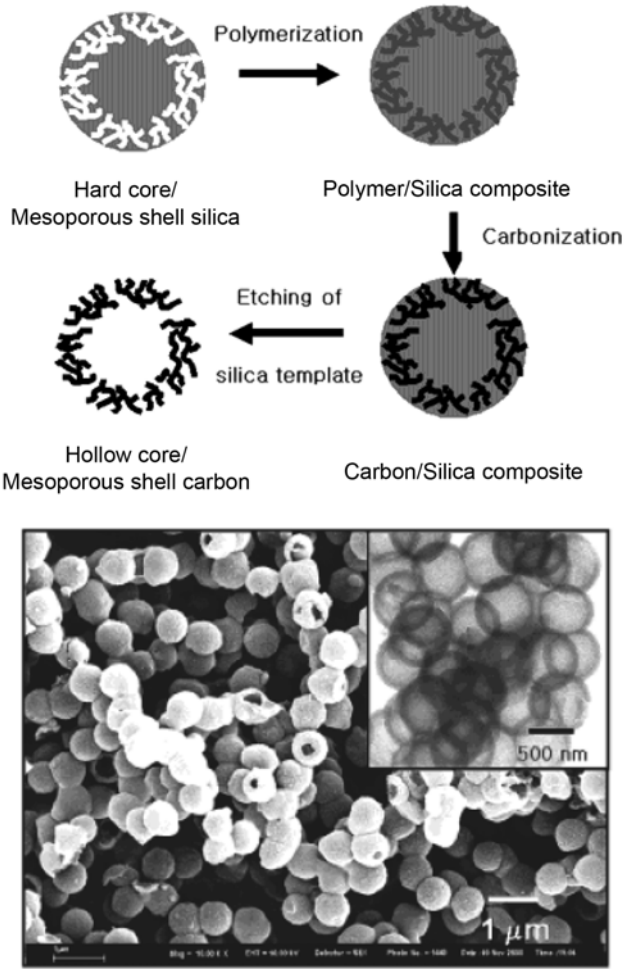

Fig. 1. (a) Schematic illustration for the synthesis of hollow core/ mesoporous shell (HCMS) carbon capsules, (b) SEM image and low-magnification TEM image (inset) of HCMS carbon capsules with core diameters of 500 nm and shell thicknesses of 90 nm [10].

with pseudo-hexagonal prismatic shape.

Layer by layer self assembly approach to fabricate many different core-shell materials was introduced by Caruso [12]. Hampsey et al. [13] reported the synthesis of spherical mesoporous carbon particles from silica templates synthesized from an aerosol assisted surfactant self-assembly process. They also reported a direct one-step synthesis of ordered mesoporous carbon via self assembly of resorcinol-formaldehyde polymer and surfactant in aqueous phase in the presence of glutamic acids as a catalyst. The process has the advantage of being a single step self assembly process that only involves the use of simple organic precursors and water. Hydrothermal carbonization of carbohydrates represents a cheap, easy and green substitute for the production of carbon sphere [14].

Onion-like carbon material was first found by Iijima at the surface of graphite electrodes [15] and interest developed after 1992. Ugarte [16] discovered a reproducible technique to synthesize onion-like carbon material that consists of irradiating carbon soot by an intense electron beam. Zheng et al. [17] reported the high temperature synthesis of carbon onion with larger quantities of amorphous carbon by chlorination of TiC powder at 1,173 K. Carbon onions with diameters ranging from 5 to 50 nm have been synthesized on a mass scale by CVD over a Ni/Al catalyst at 873 K. They are graphitic and have polycrystalline structures; this work provides a practical and convenient route for the future production of carbon onions [18]. TEM image of the as prepared carbon onions is shown in Fig. 2.

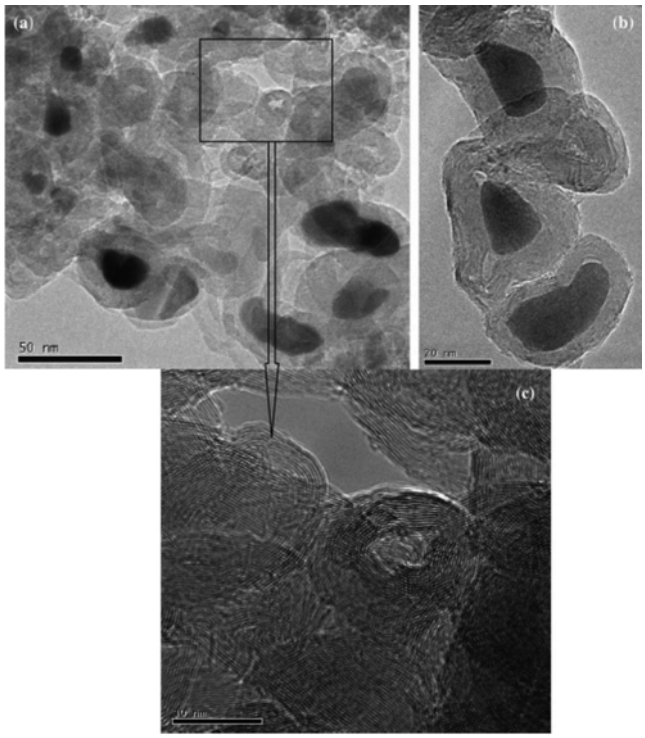

Fig. 2. TEM image of the as prepared carbon onions [18].

2. Surface Modification

Porous carbon material with a variety of structure requires surface modification when applied in separation, catalysis and energy storage. Chemical modification of the carbon is difficult, due to low reactivity of carbon. Hence, the incorporation of functionality in porous carbon during their synthesis is the efficient way. The suitable precursors include nonaromatic compounds and heteromatic compounds such as the compounds containing the N, S, O (e.g., Pyrrole, furan, thiophene, etc.) which are reported [19].

Nitrogen can be introduced in carbons essentially in two ways, either by carbonizing nitrogen containing organic compounds or mixtures of nitrogen containing precursors with nitrogen materials or high temperature treatment of carbon materials with nitrogen containing gases by which decomposition has taken place and formed the highly reactive radicals.

Kawabuchi et al. [20] reported the deposition of an aromatic compound like pyridine on the commercially activated pitch-based carbon fiber (ACF) with slit-shaped pores. The deposition was performed at 998 K for pyridine and 973 K for pyrrole. Yang et al. [21] applied a similar hypothesis to introduce the nitrogen-containing impurities into pore wall of ACF by treatment of pyridine in helium stream in the temperature range of 973 K to 1,273 K, with the intention to produce the hydrophobic sites. Pyrrole is another suitable candidate as a CVD precursor for nitrogen-doped mesoporous carbons, having a relatively high pressure even at room temperature [6]. Yang et al. used a mesoporous silica template which is im-

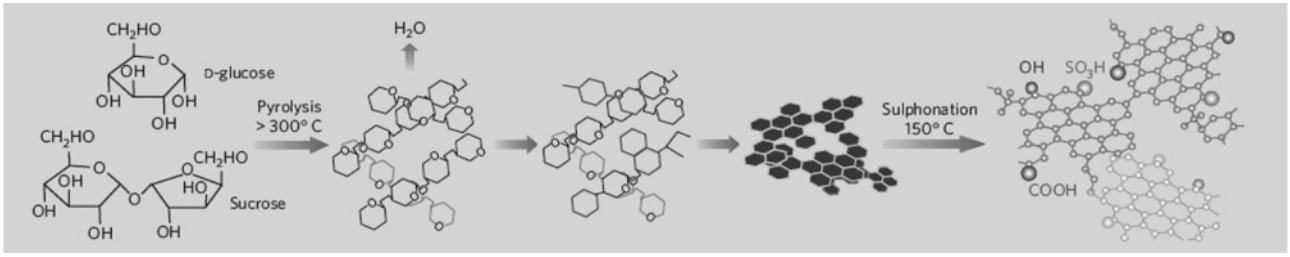

Fig. 3. Preparation from sucrose and D-glucose of a solid catalyst suitable for biological diesel production [32].

pregnated with $FeCl_3$ as the oxidant for formation of polypyrrole. Because oxidative polymerization is stoichiometric between pyrrole and $FeCl_3$, the loading of polymer and subsequently, carbon, is readily controlled [22]. Chemical vapor deposition (CVD) permits easy penetration of volatile precursors into the pores of a hard template, whether they are small micropores like zeolite templates or larger mesopores like mesoporous silica templates. Haley [23] introduces pyridine groups by cyclotrimerization of diethynylpyridines with various substitution patterns within mesoporous silica, acting as a hard template.

Vinu et al. [24] reported nanocasting of mesoporous carbon nitride samples by polymerizing and pyrolyzing a mixture of ethylenediamine and carbon tetrachloride within the pores of SBA-15 and SBA-16. The degree of polymerization, and hence textural parameters, were controlled by varying the ratio of carbon to nitrogen in the nitrogen source. An alternate nitrogen-doped carbon precursor, melamine-formaldehyde, was used for nanocasting mesoporous carbon spheres from fumed silica particles [25]. Urea is another source as a nitrogen precursor. Rideal and Wright got a success for activated carbon doping by impregnating them with urea solution [26]. The activation with ammonia and its effect on the pore structure of the carbon has been described repeatedly [27]. There are some other techniques for introduction of nitrogen into carbons by heating with hydrogen cyanide or cyanogens gas [28]. The quantity of nitrogen introduced is smaller than when NH_3 is used but the other results are similar.

2-1. Sulfonation

Budarin et al. [29] synthesized mesoporous carbon by carbonization of starch, and polysaccharide was sulfonated by suspension in sulfuric acid at elevated (high) temperature. The resulting product content was 0.5 mmol g^{-1} sulfonate concentration, which can provide high conversion, selectivity, and reaction rates for several catalytic reactions. Wang et al. [30] carried out the functionalization of ordered mesoporous carbons with sulfonic acid groups by reduction of a diazonium salt, 4-benzene-diazoniumsulfonate, by hydrophosphorous acid; this method provided a coverage of 1.93 mmol g^{-1} under relatively mild conditions, and the product was successfully used as a catalyst for esterification and condensation reactions. These kinds of sulfonated porous carbon materials offer significant potential as an environment-friendly solid acid catalysts that may be a good substitute for homogeneous or liquid acids in certain catalytic reactions, overcoming the disadvantages regarding homogeneous catalyst and reused repeatedly after regeneration.

Shin et al. [19] has applied Fridel-Crafts alkylation for the preparation of sulfur functionalized carbon by nanocasting using linear polymerization of 2-thiophenemethanol. Toda et al. [31] synthesized a heterogeneous catalyst for esterification of higher fatty acids by sulfonating incompletely carbonized natural organic material. Sulfonation of this material would be expected to generate a stable solid with a high density of active sites, enabling a high-performance catalyst to be prepared cheaply from naturally occurring molecules. First, D-glucose and sucrose are incompletely carbonized at low temperature to induce pyrolysis and the formation of small polycyclic aromatic carbon rings, sulfonite groups ($-SO_3H$) are then introduced by sulfuric acid. The scheme they use to sulfonate incompletely carbonized saccharides is shown in Fig. 3.

2-2. Halogenations

Halides are introduced into carbon for surface modification to change the chemical and physical properties of carbon materials. Fluorination is used to create a hydrophobic carbon surface. Fluorination on the carbon surface has been done by a variety of methods. Li et al. [32] reported the fluorination on mesoporous carbons by flowing diluted F_2 gas over the sample for four days at different temperatures ranging from RT to 523 K. In this method, fluorine gas reacts with hydrogen atoms in C-H bonds, and also with unsaturated bonds of the carbon. Fluorine amount can vary in accordance with the reaction conditions. TEM image of a fluorinated mesoporous carbon material prepared at room temperature is shown in Fig. 4.

Wang et al. [33] synthesized the mesoporous carbons modified with fluoroalkylsilane by hydrolysis. The functionalized carbon is super-hydrophobic, exhibiting a very high water contact angle and low water adsorption. Boehm mentioned in his review that halogenation of carbon blacks with bromine (and also chlorine) is possi-

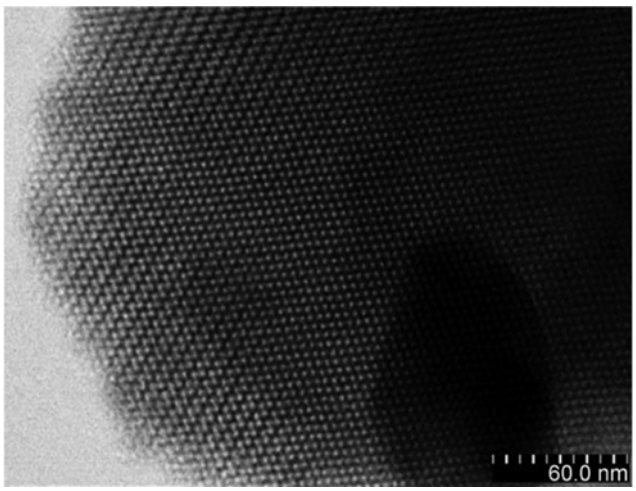

Fig. 4. TEM image of a fluorinated mesoporous carbon material prepared at room temperature [33].

ble by high-temperature treatment with the halogen [34]. Modified surface by halogenation provides a starting point for subsequent conversion into other functional groups, such as amines, anilines, alcohols, or thiols. Pitch-based ordered carbon with fluorine could be fluorinated at room temperature or moderately elevated temperature, which has great potential applications in electrochemistry or batteries [32]. When the rayon-activated carbon fiber was modified by chlorine or bromine, its surface hydrophilic property was increased and the adsorption capacity of dimethyl sulfide was increased [35].

2-3. Surface Oxidation

The heteroatoms on the surface of activated carbon play significant role in its application. Among these heteroatoms, the oxygen-containing functional groups (also denoted as surface oxides) were the widely recognized and the most common species formed on the surface of carbons, which significantly influenced their performance in sensors, energy storage and conversion systems, catalytic reactions and adsorptions. The surface oxygen-containing functional groups could be introduced by mechanical [36], chemical and electrochemical routes [38]. Oxidative treatment is the most frequently used method to functionalize the carbon surface. When functional groups are not included directly during the synthesis of porous carbon materials, controlled oxidation may be used to introduce oxygen-containing groups such as esters, carboxylic acids, phenol, lactones, ether, etc. on the carbon surface. Acidic groups such as carboxylic acid, phenolic hydroxyl, quinine and lactones are introduced to porous carbons treated with different oxidizing solution [38]. Those form a surface complex leading to change of surface chemistry, which is reflected in improved properties when carbon material is used as catalyst or adsorbent [39].

Generally, oxidation can be done by dry or wet oxidation, plasma treatment and electrochemical modification. Wet chemical oxidation involves the use of nitric acid, sulfuric acid, phosphoric acid, alone or in combination with hydrogen peroxide, sodium hypochlorite, Pradhan et al. [40] functionalized activated carbon with surface oxygen complex through the reaction with different oxidants like dil. nitric acid, hydrogen peroxides and saturated solution of $(NH_4)_2S_2O_8$ in 4 M sulfuric acid.

Nitric acid treatment is the most effective in terms of modifying the surface area and the porosity of activated carbons. Oxidation with nitric acid is a highly efficient process for the generation of surface functional groups and is quite controllable, simply by tuning the temperature, concentration and period; for this reason this oxidation technique has also been applied successfully to the surface of mesoporous forming carboxylic group [41]. Vinke et al. [42] found that the nitric acid oxidation was most effective, resulting in the highest amount of acidic surface groups, whereas hypochlorite appeared to be a much weaker oxidants. Recently, Ryoo et al. [43] reported the surface modification of CMK-5 and CMK-1 by oxidation with concentrate nitric acid at 383 K. For oxidation by concentrated nitric acid, even at RT the pore structure of CMK-5 was destroyed [44], and lower oxidation temperature or lower oxidation concentration is favorable in terms of maintaining the pore structure.

In case of dry oxidation, gaseous oxidation agents like oxygen, ozone and carbon dioxide are often used. The type of oxidants influences the composition of the surface group. For example, in comparison with ozone treatment, air oxidation produced more phenol and fewer lactones/ anhydride groups [45]. Ozone as a strong oxidization agent could oxidize the carbon material surface to introduce oxygen-containing groups. The ozone dose and oxidation time affected the resultant oxygen-containing groups and the oxygen concentration on the carbon surface. Activated carbon on oxidation with ozone showed that the higher the ozone dose, the higher was the oxidation of the carbon and the greater was the number of acid groups present on the carbon surface, especially carboxylic groups, whereas the pH of the point of zero charge decreased [46].

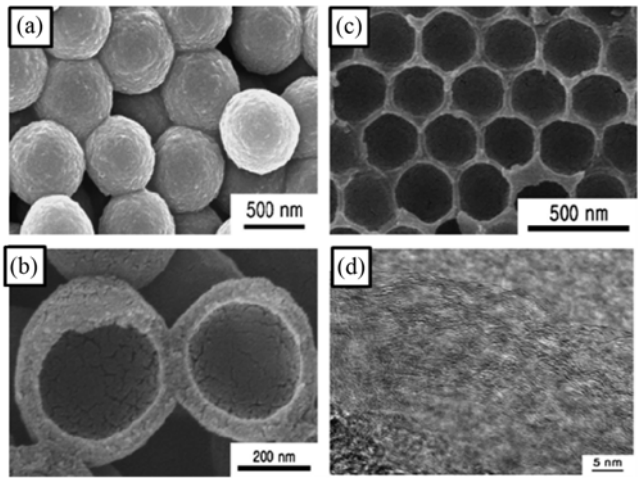

Fig. 5. SEM images of (a) CNSs, (b) NBC-1s, (c) NBC-2s, and (d) HRTEM image of NBC-2s after calcination at 1,573 K [48].

Abdi et al. [47] reported the preparation of novel carbon material having fairly uniform bowl shape in nanosize domain with varying oxygen content by a simple oxidative chopping of carbon nanoballs, where they have effectively functionalized the inert carbon nano sphere (CNS) with carboxylate groups. The lower-oxygen-containing bowls referred to as NBC-1s (O: 4.30%) were as nonclustered bowls, high oxygen- containing bowls NBC-2s (O: 30.0%) formed aggregates arranged in a honeycomb-like architecture. SEM and HRTEM of NBC-1s and NBC-2s are shown in Fig. 5.

2-4. Grafting

Grafting is another method for functionalization of carbon. Grafting of vinyl trimethoxy silane (VTMOS) improves the hydrophobicity of carbon and affinity of carbon materials towards non-polar organic solvent. Activated carbon was functionalized with VTMOS by soaking the carbon in a dilute aqueous solution of the alkoxide. This functionalization allowed better wetting of the carbon by propylene carbonate for use in electric double-layer capacitor applications [48].

Electrochemical grafting on carbon is possible with diaryliodonium salt, a process which has been demonstrated for glassy carbon electrode [49]. The approach is based on the reduction of iodonium salts and allows the co-valent immobilization of aryl groups as well as alkynyl group. The functional group attached by this method varied from electron withdrawing to electron donating group and included carboxylic acid, bromine, chlorine, methyl and metoxy group. Delamar in 1992 first demonstrated the use of dizonium compounds to modify the surface of carbon materials including glassy carbon electrode, carbon fibers, carbon powder [50]. A variety of diazonium salts, including 4 nitrophenyldiazonium tetrafluoroborate in an acetonitrile solution, were electrochemically reduced on the surface of the car-

bon.

Another grafting approach was based on Prato's reaction, the 1,3-dipolar cycloaddition of azomethine ylides [51]. Ordered mesoporous carbon was heated in a solution containing the α-amino acid N-methylglycine and an aldehyde. This method permits simultaneous attachment of two different R-groups to the carbon surface; functionalization of highly graphitic mesoporous carbon was unsuccessful by this method.

On the surface of mesoporous carbons like CMK-1 and CMK-5, carboxyl groups generated by oxidation were reacted with thionyl chloride in order to convert them to acyl chloride groups [52]. The acyl chloride groups could then be used to attach hydroxypropyl amine onto the carbon surface by esterification.

Fig. 6 shows a summary of grafting reactions that permit functionalization of templated nanoporous carbon (TNC) surfaces with covalent anchors [43,52]. Because the starting surfaces were not

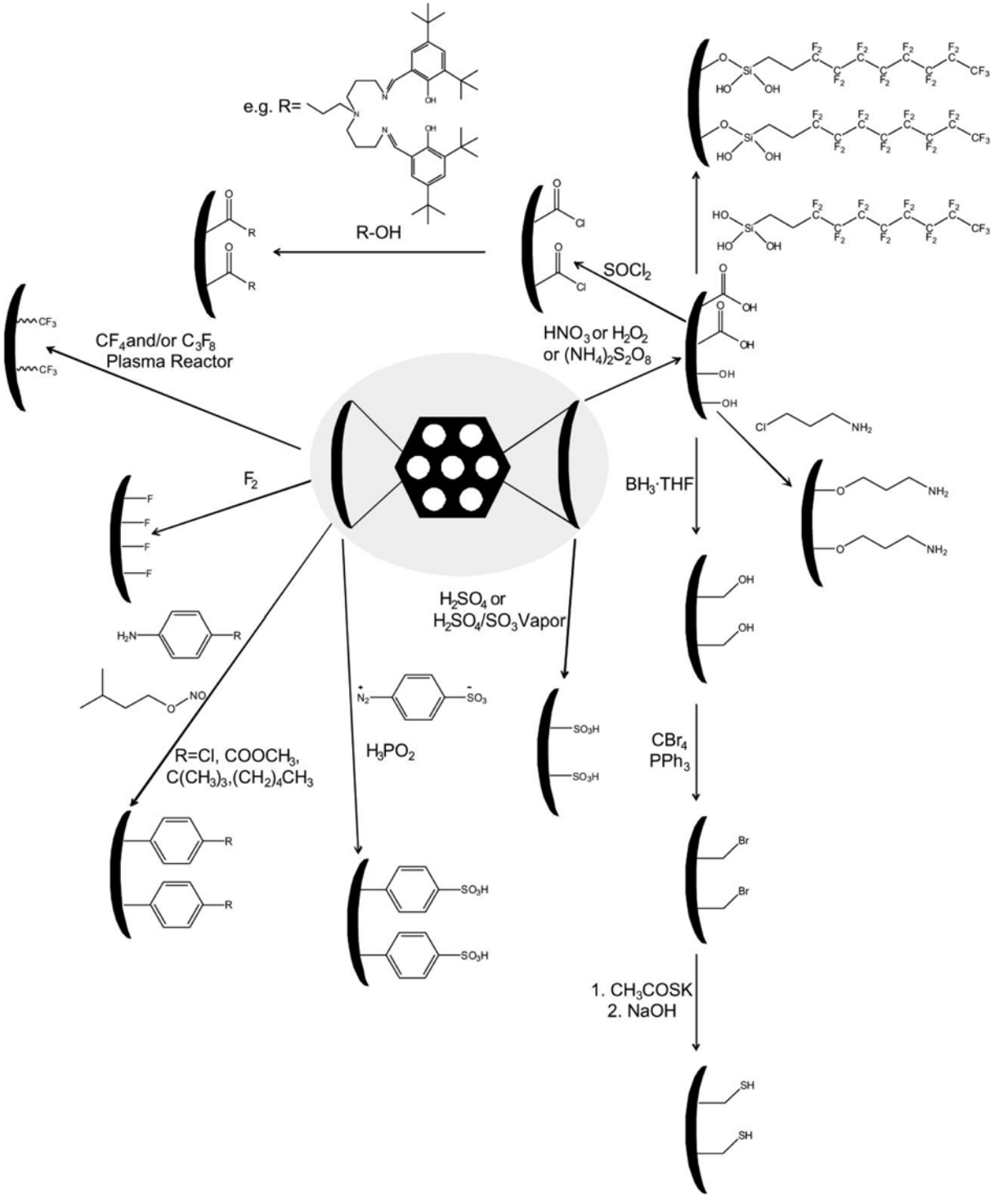

Fig. 6. Summary of grafting reactions that permit functionalization of TNC surfaces with covalent anchors [44,53].

always fully specified in the original papers, idealized surfaces are depicted here. The largest variety of surface functional groups on porous carbons is accessible by grafting techniques (Fig. 6). In some of these methods, the carbon surface has a preexisting surface functionality, and the surface functionality is changed by an organic reaction.

CHARACTERIZATION

Elemental analysis is a process in which materials or compounds are analyzed for their elemental and sometimes isotopic composition. Elemental analysis can be qualitative (to identify elements) and it can be quantitative. The most common form of elemental analysis, CHSN analysis, is accomplished by combustion analysis. Considering the application aspects, it is important and necessary to determine the surface functional groups of carbon materials. The technique of characterization of bulk, external and internal surface of surface functional groups will be discussed in this review.

1. Bulk Characterization

1-1. Solid State NMR

High resolution solid-state ^{13}C NMR spectroscopy is well known for analyses of coals and activated carbons [53]. The ^{13}C NMR spectra could determine the chemical functionalities of porous carbons. From the literature, peaks near 30 ppm, 80 ppm and 127 ppm in the ^{13}C NMR spectra could be assigned to the sp3- hybridized carbon [54], sp-hybridized carbon and sp2-hybridized carbon in graphite or graphite-like domains, respectively [55]. The peak near to 175 ppm in NMR spectra is due to alkoxy and OH substituted carbon and peak at 40 ppm could be attributed to the presence of -CH and $-CH_2$ groups and the signal at 39 ppm can be assigned as the cross-linked methylene groups [56]. The olefinic carbon atoms with a broad signal between 120 and 140 ppm were clearly detectable in the solid-state ^{13}C NMR spectrum [57]. Characterizations of complex carbonaceous structures could be done by combining data from multiple solid state NMR techniques [58]. ^{13}C cross polarization magic-angle-spinning (CP-MAS) NMR experiments provide qualitative information about the structure of carbonaceous solids, revealing, for example, aromatic and aliphatic resonances [59]. Dipolar dephasing experiments and ^{13}C CP-MAS spectral editing techniques provide accurate information about ratios of protonated and non-protonated aromatic and aliphatic carbons, respectively. 19F solid-state NMR has been applied to follow fluorination processes in porous carbon material [60]. ^{1}H solid-state NMR of carbonaceous solids is complicated by the high abundance of protons in many of these materials. It is necessary to use ^{1}H NMR techniques that eliminate the effects of ^{1}H-^{1}H dipolar interactions that lead to strong line broadening, for example combined rotation and multiple-pulse spectroscopy (CRAMPS) [61].

1-2. FT-IR (Fourier Transform Infrared) Spectroscopy

The FT-IR has been widely used to characterize the surface groups of different oxides and also applied to various types of carbon and carbonaceous materials like coals, carbon blacks, chars and activated carbon structures [62]. Since IR transmission spectra had peaked shapes where the specific chemical bonds existed, it was possible to know which functionalities were created on the surface of activated carbon by comparing locations and depths of the peak. FT-IR was mainly used as a qualitative technique for the evaluation of the chemical structure of carbon materials. It was not easy to get good spectra because carbons are black materials that absorb almost all of the radiation in the visible spectrum, and the peaks obtained were usually a sum of the interactions of different types of groups [63]. To analyze carbon surface functionalization, it is useful to compare spectra of nonfunctionalized and functionalized materials and follow the appearance and disappearance of absorption bands. Photoacoustic spectroscopy is a technique which has been used with carbon samples, but it is not commonly used [64]. In situ DRIFTS measurements have been used to study the formation of surface groups on carbon by oxidation. Some FT-IR assignments of chemical functional groups are listed in Table 1 [65-67].

Table 1. IR assignments of functional groups on carbon surfaces [66-68]

Group or functionality	Assignment regions (cm^{-1})
Carbonates; carboxyl-carbonates	1100-1500, 1590-1600
Alcohols	1049-1276, 3200-3640
-C-OH (stretching)	1000-1220
Lactones	1160-1370, 1675-1790
-OH	1160-1200, 2500-3620
-C-C aromatic (stretching)	1585-1600
C-O in ethers (stretching)	1000-1300
Quinones	1550-1680
Carboxylic anhydrides	980-1300, 1740-1880
C-H (stretching)	2600-3000
C-N	1190
Cyclic amides	646,1461,1546,1685
C=C=N	2070-2040
N-O-	1300-1000
C-N aromatic ring	1000, 1250, 1355
N-H, C=N	1560-1570

1-3. Raman Spectroscopy

Raman spectroscopy has been used to study a number of carbon-containing particles such as commercial graphite of various compositions, candle soot and diesel soot, and ambient particles. The spectra show the known D, G, D′ and 2D bands with varying characteristics. An analysis of the spectra allows the inference of internal physical characteristics of the samples such as the size or degree of disorder of the carbon microcrystalline domains on a nanometer scale [68]. Raman spectra of activated carbon materials have been investigated by a peak-deconvolution technique [69]. FT-IR and FT-Raman spectroscopy are important complementary tools for the characterization of activated carbon, because some IR-inactive vibrations can be active in Raman spectra of carbonaceous materials. Although the Raman spectrum of carbonaceous materials consists of only a small number of lines, the variations in the intensity, width and peak position of these lines are very large and their full theoretical interpretation is still a challenge.

The absorption at about 1,580 cm^{-1} (also known as G band) has been ascribed to the Raman-active optical mode E_2g of 2-dimensional graphite arising out of vibrations of carbon atoms in a hexagonal carbon lattice, such as a graphene layer. Another signal at about 1,340 cm^{-1} (also known as D band) is usually assigned to the vibrations of carbon atoms with dangling bonds at the end of disordered

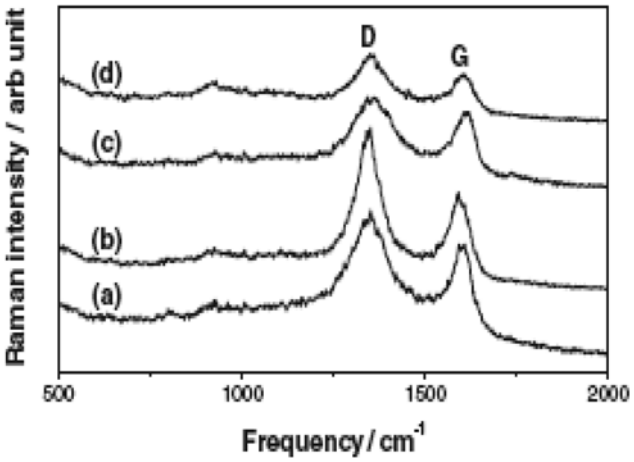

Fig. 7. (a) Raman spectra of (a) CNSs, (b) CNSs calcined at 1,573 K, (c) NBC-2s and (d) NBC-2s calcined at 1,573 K [48].

graphitic carbon. The relative intensity of the two bands with stronger G band is a reflection of the good quality of graphite-like structure while its shifting to higher positions with higher D band intensity indicates a more disordered structure. In the Raman spectra of CNSs (a) and NBC-2s (c), both the carbons gave a G band at about 1,590 cm^{-1}, indicating the presence of graphitic carbon in them. However, a strong D band at about 1,350 cm^{-1} reveals that there are considerable structural defects in both the materials [47] as shown in Fig. 7.

Since the pioneering work of Nemanich and Solin [70], much has been published on the Raman spectra of graphite and graphitic particles. The literature on the subject continues to increase, because of the wide variety of applications of these materials. The article by Wang et al. [71] provides important evidence for the understanding of the D peak and its relation to edge carbon vibrations. McCulloch et al. [72] provide a description of the shape of the G band in terms of the Breit-Wigner-Fano (BWF) function. Fig. 8 gives a detailed analysis of Raman spectra of glassy carbon (GC) and activated carbon (AC) [68].

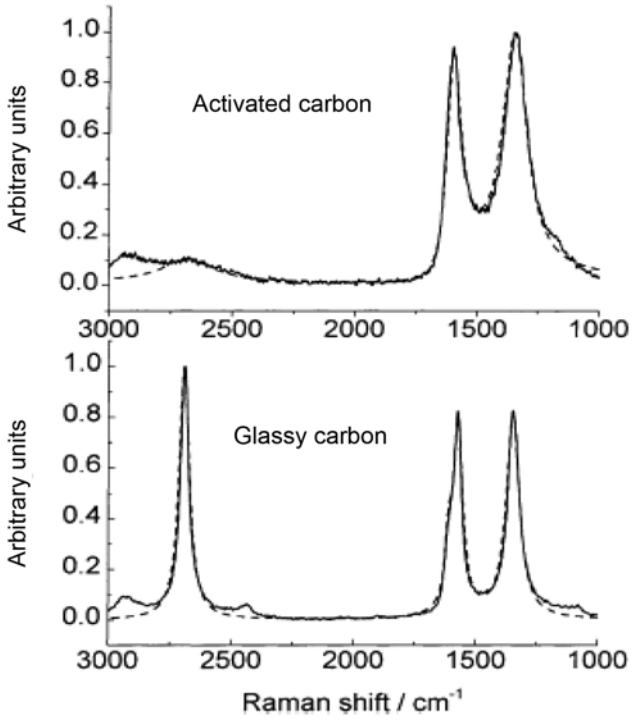

Fig. 8. Detail of analysis of Raman spectra of glassy carbon (GC) and activated carbon (AC) [87].

2. External Surface

2-1. X-ray Photoelectron Spectroscopy (XPS)

XPS is a technique for investigation of the surface functionalities of carbon materials as reported by a number of studies [73,74]. XPS can provide valuable information about the presence and amount of nitrogen groups, carbon groups, oxygen, fluorine, sodium and other components in the template carbon. The XPS spectra of C_{1S} and O_{1S} indicated that carbonyl groups were introduced to the surface at low oxidation potentials and the concentration of alcohol-ether groups increased at high oxidation potentials [75]. However, the OH and C-O oxygen atoms in the carboxyl groups could not be easily distinguished if the XPS experiments were carried out at room temperature [76]. XPS applied to characterize the composition of designed porous materials provides a compositional estimate of only the outermost layers, with a penetration depth of ca. 5-15 nm [77]. This spectroscopic method has been extensively employed to study the surface carbon-oxygen complexes and elemental composition before and after surface treatments. XPS applied to the porous carbons for the determination of the oxygen surface groups has some limitations, like the analysis was made in high-vacuum, that

Table 2. The C_{1S}, O_{1S}, N_{1S} from XPS spectra for modified norit ROW 0.8 [74,79]

C_{1S}		O_{1S}		N_{1S}	
Assignment	B.E. (eV)	Assignment	B.E. (eV)	Assignment	B.E. (eV)
-C=C-,non-functionalisedsp2C	284.5+0.1	H_2Oads, O_2ads	536.3+0.4	NOx, oxidized, N-O-C	404.5+0.4
-COOH (carboxyl acid)	289.3+0.1	COH, COOH, N-OC	534.3+0.2	N, quaternary	401.3+0.2
-C=N, -N=C-O-, COOC	288.7+0.2	C=O (ester, amides)	532.3+0.3	-O-C=N, pyridine pyrrole	400.2+0.1
-C-N, C=O	287.4+0.2	C=O (carboxyl)	530.6+0.2	-N-H	
				Pyrrolic nitrogen	399.4+0.3
				Pyridine nitrogen	
– C-OH, .C-O-C=, C-O-R	286.1+0.1	C-O-C (ester oxygen)	533.5+0.2	Pyridinic nitrogen, Ar-N-Ar	398.6+0.3
Plasmon	292.0+0.4			Pyridine-N-oxide	402.5-403.8

is, under conditions quite different from those usually used in the applications of the carbon catalyst, rearrangement of the surface can occur and deconvolution of the O_{1S} and C_{1S} peaks is not straightforward, the external surface area is only a small fraction of the total surface area and it is not representative of all of the material.

The binding energy and their assignment of C_{1S}, O_{1S}, and N_{1S} deduced from XPS spectra for modified Norit ROW 0.8 are summarized in Table 2 [73,78].

3. Internal Surfaces

3-1. Temperature-programmed Desorption (TPD)

TPD is a thermal analysis method that is widely used for the characterization of the oxygen-containing groups of activated carbons [77,79]. Oxide-containing functional groups decompose in specific temperature ranges to produce CO, CO_2, or H_2O as decomposition products. The nature of the groups could be estimated by the decomposition temperature and type of gas desorbed and their respective amounts by the areas of the peaks. The major problem is the difficulty in identifying each surface group individually because TPD spectra showed composite CO and CO_2 peaks. A differential scanning calorimeter and a thermogravimetric analyzer (DSC-TGA) coupled to a mass spectrometer [40] were used for the analysis of surface group on carbon materials. Surface oxygen-containing groups on carbon and their decomposition by TPD are illustrated in Fig. 9 [77,79].

Temperature-programmed reduction (TPR) is a similar technique to study the reactivity of surface functional groups upon sample heating in a reductive atmosphere [80].

3-2. Chemical Titration

The surface acidity of several activated carbons was evaluated using the Boehm and potentiometric titration methods. The chemical titration method proposed by Boehm [81] were especially useful when it was used in combination with other techniques [82]. Oxygen-containing groups, like ketones, phenols, lactones, lactol, carboxylic acids, and carboxylic anhydrides can be categorized by adsorption neutralization with $NaHCO_3$, Na_2CO_3 and NaOH solutions, respectively [83]. The acid dissociation constants of carboxyl groups, lactones, or phenols differ by several orders of magnitude. pH measurements show the carbon to be highly acidic, with Boehm titration and XPS suggesting a high proportion of carboxylic and lactonic surface groups. The basic group (such as, C-H, C=N groups, amino, cyclic amides, nitrile groups) contents of the activated carbons were determined with 0.05 M HCl [84]. Redox titrations (e.g., with Ce (IV) solutions) allow detection of reducing groups that may have been introduced into the porous carbon during thermal treatment under reducing conditions [85].

When dealing with small amounts of sample, problems of reproducibility occur due to very long equilibrium times for porous carbon material and the Boehm titration method only can determine about 50% of the total oxygen available in activated carbons; these are the limitations of the traditional Boehm titration method [86].

3-3. X-Ray Diffraction and Small-angle X-ray Scattering

X-ray diffraction technique is used by solid state chemists to examine the physico-chemical make-up of unknown solids. In the porous carbon material mesostructural periodicity, pore structure and unit cell parameters of mesoporous carbon can be determined. Use of 2D transmission X-ray diffraction, grazing angle X-ray diffraction are more appropriate to characterize the channel orientation in mesoporous films [87]. Bulk nanoporous carbon materials are produced

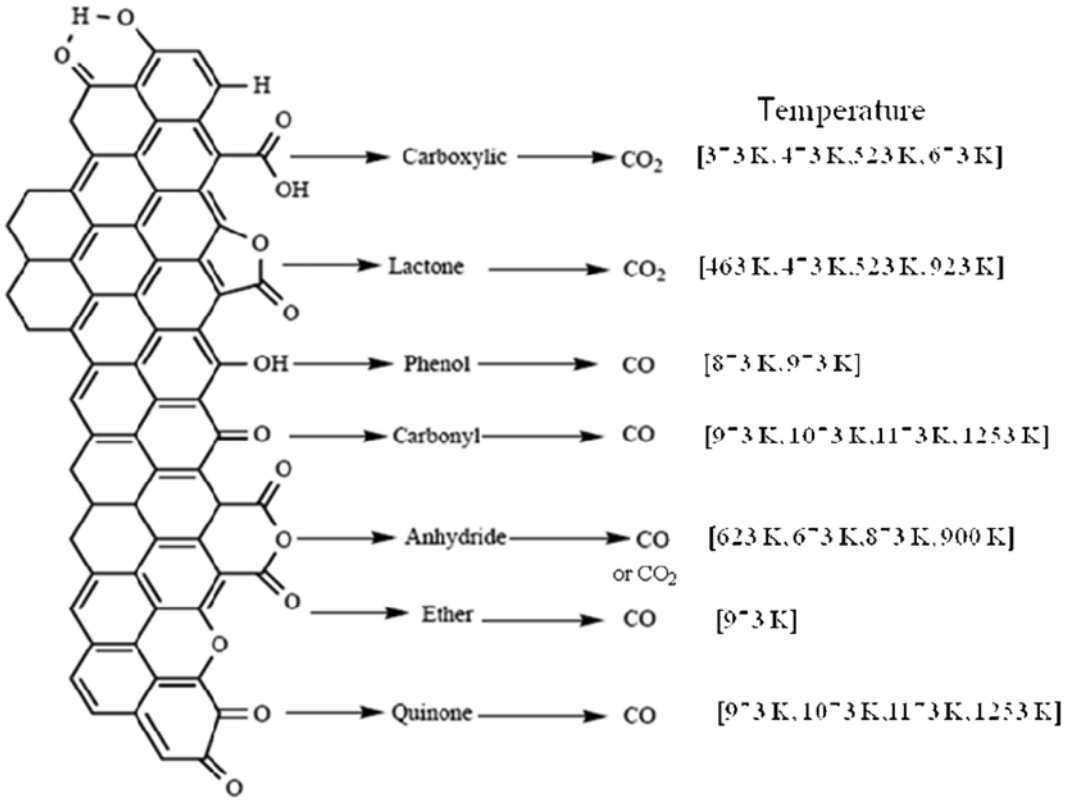

Fig. 9. Surface oxygen-containing groups on carbon and their decomposition by TPD [78,80].

from a number of carbides by selective etching reaction with chlorine, and these studies were carried out by the techniques of small angle X-ray scattering [88]. The porous structure of carbon-graphite materials styrene-divinylbenzene copolymer and fruit stones has been studied by means of X-ray small angle scattering method. The main parameters of porous structure like inertia radius, pore size distribution functions, and specific surface area have been determined [89]. Information regarding successful filling of pores with functional groups can also be derived from X-ray diffraction data, by analyzing relative peak intensities before and after surface functionalization [90]. Hollow porous carbon nanospheres with large surface area and stability were self-assembled using gentle oxidization of fullerenes. The C_{60} framework, functional groups, composition, structure of the nanospheres were investigated [91].

3-4. Gas Sorption Isotherms

Gas adsorption is a prominent method for obtaining a comprehensive characterization of porous materials with respect to the specific surface area, pore size distribution and porosity [92]. Amorphous materials are typically characterized using nitrogen adsorption isotherms at 77 K to obtain pore size distributions. However, higher temperatures and different adsorbates could also be used. In mesoporous carbons, specific surface areas are calculated from the isotherms by means of the BET method and the new α_s-method [93]. Total pore volumes may be calculated by a single-point measurement at a high relative gas pressure (p/p^0=0.98), micropore volumes by applying the Dubinin-Radushkevich analysis on the isotherm in a low relative pressure range (10^{-4} to 10^{-2}) and volumes of pores <1 nm by the Horvath-Kawazoe (HK) method applied to the relative pressure range from 10^{-6} to 10^{-4}. Adsorption of CO_2 at 295 K on a variety of microporous carbons was analyzed using the Dubinin Radushkevich (D-R) equation [94].

Recently, Jaroniec [95] has extended to nitrogen and argon-sorption isotherms of carbonaceous materials with cylindrical mesopores in the pore-size range from 1 to 12 nm. Neimark et al. [96] present a unified approach to pore size characterization of microporous carbonaceous materials such as activated carbon and carbon fibers by nitrogen, argon and carbon dioxide adsorption at standard temperatures, 77 K for N_2 and Ar and 273 K for CO_2. Reference isotherms of N_2, Ar and CO_2 in a series of model slit-shaped carbon pores have been calculated from the nonlocal density functional theory.

APPLICATIONS

Carbon materials are used in many applications such as catalyst, Li-ion batteries, energy storage, sensing and sorption due to their chemical stability, electronic conductivity, ability to intercalate electrochemically active species, and sorption capabilities. Generally, glassy carbon and graphitic carbon are used for electrodes and activated carbons are used for catalysis and sorption. In this section we will highlight applications of porous carbons with a particular emphasis on the effects of carbon functionalization on each application.

1. Catalysis

Commercially available carbon-supported materials are well known as heterogeneous catalysts, for a variety of reactions such as hydrogenation, dehydrogenation, oxidation, hydrodesulfurization, hydrodenitrogenation, hydrodeoxygenation, electrocatalytic reactions and NO reduction [90]. This is due to their desirable properties such as chemical inertness, stability in the absence of molecular oxygen at high or low pH values, mechanical resistance and high surface area. Surface areas and pore size distribution are most important major factors in catalytic reactions involving large molecules, where accessible mesopores are preferred over micropores [39]. Ion exchange, impregnation, colloid dispersion, electroless plating, or vapor-deposition methods, are the typical preparation methods for metal loaded functionalized carbon. The control of the carbon surface chemistry (surface oxygen and other heteroatoms, amphoteric character and hydrophobicity) is very important for control over the pore structure of carbon supports [41].

In the last few years, a few studies have been reported for functionalized carbon. Mesoporous carbon accounted more advantages like good dispersion, adsorption of reagent and desorption of product. But the activity and selectivity depend on how well the placement of catalyst particles and their size distribution can be controlled. Lee et al. studied the bifunctional Co-Mo catalyst loaded nonporous resorcinol-formaldehyde-based carbon catalyst and activated carbon catalyst for hydrosulfurization reaction; the turn-over frequency was lower in case of activated carbon due to blocking of pores by metal particles. These things should not be happening in case of nonporous carbon because of lesser diffusion limitation for reagent and the catalyst particle not obstructing the pore opening [97].

Zhou et al. [98] synthesized the Pt loaded on modified mesoporous carbon with cationic surface (cetyltrimethylammonium bromide) by microwave-assisted synthesis for hydrogen electro-oxidation study. For results, the wettability of the carbon was enhanced, the Pt loading increased and Pt nanoparticles were well dispersed throughout the mesopore system, which has been shown as effective during reactions. Ryoo et al. [99] reported the need of lower Pt loading on mesoporous carbon than activated carbon support for selectively biphasic conversion of nitrobenzene to p-aminophenol. The result was attributed to the higher catalyst dispersion on the mesoporous supports and the lower pore diffusion resistance in these structured materials.

Harada et al. [100] compared the activity of Pd-loaded ordered mesoporous carbon (Pd-CMK-3), Pd-loaded activated carbon and Pd-loaded carbon black for oxidation of benzyl alcohol; the conversion and selectivity towards oxidation of benzylalcohol into benzaldehyde do not necessarily benefit from the ordered mesostructure. The conversion was seen highest with Pd-carbon-black, and selectivity was in fact the lowest for Pd-CMK-3. Instead of the pore architecture, the size and dispersion of Pd particles had a greater effect on the catalytic functions. The conclusion is that Pd particles were located on the external surface of CMK-3 and the reactions were therefore not significantly influenced by the mesopore structure, and if Pd is dispersed on a molecular level within the mesopore walls, very high selectivities and conversions can be obtained. It should be noted that good metal dispersion does not always lead to the expected performance advantages. In some cases the catalyst with lower metal loading should give the benefits; for example, when a mesoporous carbon xerogel prepared from resorcinol-formaldehyde precursors was activated in oxygen, impregnated with a Pd salt, reduced using sodium formate or hydrogen and then tested as a catalyst for enantioselective hydrogenation of isophorone and of (E)-2-benzylidene-1-benzosuberone [101]. Pd particle size and dispersion

were strongly influenced by the choice of reducing agent.

Synthetic carbon is a useful support for acid catalysis. Wang et al. [30] synthesized the hexagonally ordered mesoporous carbon CMK-5 functionalized with sulfonic acid groups by covalent attachment of sulfonic-acid-containing aryl radicals and examined as an acid catalyst for the formation of bisphenol-A and for esterification of acetic acid with ethanol.

The superior catalytic performance was ascribed in part to the hydrophobic nature of the support, which may synergistically influence the catalytic activity of the hydrophilic surface groups. StarbonR materials (a new family of mesoporous carbonaceous materials derived from renewable bioresources denoted as StarbonR) with sulfuric acid, the products become highly active catalysts for esterification of diacids, liquid phase acylation of alcohols and alkylation of aromatic substrates which can be derived by low-temperature carbonization of starch [29].

There are many reports in literature for esterification of high molecular weight carboxylic acids like oleic acid, stearic acid etc. by using sulfuric acid and solid acid catalyst. One might anticipate that the addition of uniform mesopores to such a material could bring additional performance advantages. Hara et al. [103] synthesized the sulfonated carbon by incomplete carbonization of sulfonated aromatic compounds, such as naphthalene. Even though the product obtained in a study using this approach was amorphous and had a relatively low surface area, it presented a high density of sulfonic acid groups and rivaled the performance of sulfuric acid as a catalyst for esterification of acetic acid.

2. Li-ion Batteries

A variety of advanced techniques demand rechargeable lithium-ion batteries with high energy and high power density. Generally, carbon materials, especially graphite, have been investigated for lithium-ion battery anode materials for quite some time, due to their ability to intercalate lithium ions. Commercial lithium ion batteries often employ graphitic carbon anodes which provide a theoretical capacity of 372 mA h g^{-1} [103,104]. However, new compact and modern portable electronic devices as well as hybrid electric devices require higher energy density power sources with improved cyclability and rate capability.

Ng et al. [105] recently reported that amorphous carbon-coated Si nanocomposites prepared by a low-temperature spray pyrolysis technique were used as high capacity anode material for rechargeable Li-ion batteries. In these cases, carbon-based materials have exhibited advantages as a host matrix. During Li insertion and extraction, carbon materials can buffer the volume changes of silicon particles and guarantee good electrical contact. Cakan et al. [106] synthesized carbon/silicon nanocomposites for lithium storage performance using hydrothermal carbonization of glucose in the presence of preformed silicon nanoparticles with particle size of 20-50 nm. To improve the stability and electrical conductivity of the nanocomposite, after hydrothermal carbonization, the particles were further carbonized at 1,173 K for 2 h in an N_2 atmosphere. They carried out galvanostatic charge-discharge experiments to evaluate the electrochemical performance of the C/Si nanocomposite. For comparison, a commercially available nanometer-sized Si was also tested. The discharge (Li insertion)/charge (Li extraction) curves of the C/Si nanocomposite electrode were obtained in 1 M $LiPF_6$ EC-DMC electrolyte solution containing 2 wt% vinylene carbonate at a current density of 300 mA g^{-1}. The C/Si nanocomposite showed Vs Li/Li^+ highly stable reversible capacity (~460 mA h g^{-1}) at a high current rate of 300 mA g^{-1} in the voltage range of 0.05 to 1.2 V, which is remarkably higher than that of pure hydrothermal carbon under the same electrochemical conditions.

Tin-based materials have attracted particular interest as negative electrodes because they can, in principle, deliver much higher specific lithium storage capacities (790 mA h g^{-1} for SnO_2; 990 mA h g^{-1}) than the currently used graphite materials (372 mA h g^{-1}) [104, 105]. However, the practical use of tin-based anodes is significantly hampered by the poor capacity retention over long-term charge-discharge cycling [107]. This is one of the well-known problems for anode materials based on the Li-metal alloying/dealloying mechanism that has been due to the large volume change of electrode materials accompanying Li insertion and extraction (e.g., the volume change is more than 200% when Sn alloys with Li to form $Li_{4.4}Sn$).

Han et al. [108] reported hierarchical anode nanostructure SnO_2/carbon composite hollow spheres. In these structures, the mesoporous SnO_2 hollow spheres are embedded in 3D carbon networks. Carbon hollow spheres are able to deliver a reversible Li storage capacity of 473 mA h g^{-1} after 50 cycles, which is about 27% higher than the theoretical capacity of graphite 372 mA h g^{-1}. From the literature, the capacity of the pure SnO_2 anode tends to fade quickly after 30 cycles to a value below 372 mA h g^{-1}. It should also be noted that the capacity of the SnO_2/carbon composite anode is comparable to that of SnO_2 in the course of the first 30 cycles, despite the fact that one-third of its mass is composed of low-activity amorphous carbon.

Wang et al. [109] synthesized hollow carbon spheres by CVD deposition of carbon onto silica spheres followed by silica removal. The crystalline hollow carbon spheres were subsequently decorated with SnO_2 and upon carbon removal, hollow SnO_2 spheres were produced. They compared the capacity and cyclability of electrodes of SnO_2-modified carbon spheres with electrodes of carbon spheres and SnO_2 spheres. The hollow carbon spheres showed good rate capability and cyclability. The SnO_2-modified carbon sphere particles showed a higher specific capacity and did not have the loss of cyclability often seen for SnO_2 materials. These results are due to the crystallinity of the carbon spheres and to their hollow structure, which allows for high surface area, short diffusion path lengths and recapture of SnO_2 particles that detach from the inside of the spheres. And also SnO_2 spheres had a specific capacity higher than the theoretical value of SnO_2, probably due to lithium storage within micropores between spheres or in the cavities of the hollow spheres.

Fan et al. [110] synthesized ONTC (mesoporous carbon ordered nanostructured tin-oxide-carbon composite) in which tin-based oxides were deposited into the pores of the carbon. They examined the charge and discharged capacity of ONTC with nano-SnO_2 (templated with the surfactant P123) and nano-MTBO (mixed tin oxides templated with P123). They found that the discharge capacity of ONTC was higher, and the irreversible capacity loss was high for both. The capacity fade for ONTC was smaller than either of the other two materials, with capacity retention of 42.8%. The authors concluded that the higher reversible capacity was probably due to the carbon template, which helped prevent large volume changes of the tin oxides and aggregation of the Li-Sn alloys, and provided

an electrical contact between the tin composites.

Three-dimensionally ordered macroporous carbon (3DOM) was used as the basis for an interpenetrating electrochemical cell. Ergang et al. [111] prepared 3DOM carbon anode by use of thin, conformal polymer separator and remaining pore volume was then filled with a xerogel or ambigel vanadia cathode, before or after electrochemical lithiation, respectively. They studied the charge discharge capacities of these systems. This resulted in a xerogel system which cycled at 1 mA, showing an initial discharge capacity of 70 mAh g^{-1}, which decreased to 0.7 mAh g^{-1} by the 100th cycle. The reversible capacity of the system was greatly improved with ambigel cathode, to 350 mAh g^{-1}, even at ten times greater current. Pan et al. [112] functionalized the carbon surface with multilayers of nitrophenyl groups or 4-aminobenzoic acid groups and it helped to suppress the decomposition of solvent at the electrode surface without imposing a negative effect on the lithium transfer.

3. Capacitor/Supercapacitor

Supercapacitors, as energy storage devices with a high energy density, great power density and long cycle life, are of great interest in hybrid electrical vehicles, digital telecommunication systems, computers and pulsed laser system, etc. Nowadays, the use of porous carbon-based capacitors has seen a huge demand for electrochemical capacitors and supercapacitors, in which charge is stored within the double layers at the interfaces between the carbon electrodes and the electrolyte. Supercapacitors fall into two categories: electric double-layer capacitors (EDLCs) and redox pseudocapacitors. The energy stored in carbon-based supercapacitors involves charge separation at the carbon/electrolyte interface, which leads to an electric double layer capacitance, and the presence of functional groups at the surface of carbons leads to a pseudo-capacitance. The common methods for increasing capacitance of the carbon electrode materials focus on the preparation of high-surface-area carbons with appropriate pore size and surface modification of carbons. The double layer capacitance is directly co-related with the surface area of the carbon, while the pseudocapacitance arises from sites containing redox active surface functional groups, such as quinone and hydroquinone, which are rapidly oxidized and then reduced, as the potential is changed [113]. For pseudocapacitors, metal oxide [114] and conjugated conducting polymers, such as polyaniline, polypyrrole and polythiophene have been investigated for use as electrode materials. The most beneficial metal oxide known to give very high capacitance is RuO_2. Some of the oxides which have been studied as super capacitor electrode material are NiO, $Ni(OH)_2$, MnO_2, Co_2O_3, FeO, TiO_2, V_2O_5 and MoO_x. None of these oxides are used in commercial production of EDLCs and they are still in lab-scale research. Manganese oxides are seen to be potentially useful materials for pseudocapacitors not only due to their low cost but also to their environmental friendliness [115].

Due to the existence of several different oxidation-state structures of these redox-active species over a potential range, high faradaic pseudocapacitance can be obtained. An important parameter in characterizing potential capacitor materials is the specific capacitance (F/m^2), which depends on the surface density of redox active functional groups and is independent of surface area. Gravimetric capacitance (F/g) takes into account both double layer capacitance (surface area) and pseudocapacitance (functional groups) [116]. Electronically conducting polypyrrole has attracted much attention as an electrochemical capacitor electrode material due to its unique characteristics like facile synthesis, thermal and chemical stability and environmentally friendly features [117].

EDLCs are being studied extensively due to the increasing demand for new energy-storage media with high specific power and improved durability [118]. As compared to conventional capacitors, EDLC has high power densities and relatively high energy densities, and also because of high surface area material, helps for charge accumulation and an interconnected porous network with sufficient pore windows for electrolyte wetting and rapid ionic transport. With the above concerns, mesoporous carbon electrodes, with their more accessible porous infrastructure, are promising materials for EDLC applications. EDLCs are of great interest for hybrid power sources for electrical vehicles, digital telecommunications systems (e.g., cell phones, personal digital assistants (PDAs), uninterruptible power supplies for computers and pulse-laser generators.

CONCLUSION

The discovery of nanostructured carbon materials has led to a big effort in their synthesis, preparation/purification. While tremendous progress has been made in syntheses of porous carbons with different structure, challenging opportunities remain for functionalizing such materials to optimize their properties for specific applications. In this review, an overview was provided of various methods of synthesis of core shell structure via template synthesis method and its modification. Modification of porous carbon via acidic, thermal treatment was not by far, the most studied technique, which might be attributed to its simplicity and availability of oxidization process. Generally, oxidization treatment of porous carbon was favorable for enhancing its adsorption for polar molecules, while thermal treatment was desired for adsorption for non-polar molecules. The nitrogen functional groups could improve adsorption for odor gases and acidic molecules. These methods could change the pore structure of porous carbon in little or large degree. Surface polarity is a critical consideration not only for host-guest applications but it also influences the propensity of the material for further functionalization. Super hydrophobic properties can be achieved through fluorination. Creating functionalities on carbon surfaces through oxidation requires extremely harsh chemical treatments, which can damage the integrity of both chemical and porous structures. The functionalization of carbon surfaces by either chemical or electrochemical reduction of adsorbed diazonium salts presents an alternative approach. This approach confers a high coverage of functional groups on carbon surfaces.

With respect to applications, functionalized porous carbons promise tremendous benefits over traditional carbon systems, particularly for high-value applications. For catalysis, the new carbon systems provide ways to improve the selectivity of a catalyst, enhance metal dispersion or coverage of other active groups and increase the overall activity of the catalyst. Porous carbon materials have been investigated for lithium-ion battery anode materials. Many novel and simpler technologies are still developing to meet new application demands. We may also see further incorporation of designed porous carbons into biosystems. The quantity of surface chemical functional group control and certain group introducing is still a challenge for porous carbon surface.

ACKNOWLEDGEMENT

This research was supported by MOCIE through the Institutional Research Program (KK-1101-A0).

REFERENCES

1. A. Yehaskel, *Activated carbon manufacture and regeneration*, New Jersey, Noyes Data Corporation, 51 (1978).
2. M. L. Schipco and B. N. Kunznetsov, *Fuel*, **74**, 751 (1995).
3. M. T. Gilbert, J. H. Knox and B. Kaur, *Chromatographia*, **16**, 138 (1982).
4. R. Ryoo, S. H. Joo and S. Jun, *J. Phys. Chem. B.*, **103**, 7743 (1999).
5. L. Zhou, H. Li, C. Yu, X. Zhou, J. Tang, Y. Meng, Y. Xia and D. Zhao, *Carbon*, **44**, 1601 (2006).
6. C. M. Yang, C. Weidenthaler, B. Spliethoff, M. Mayanna and F. Schueth, *Chem. Mater.*, **17**, 355 (2005).
7. D. Kawashima, T. Aihara, Y. Kobayashi, T. Kyotani and A. Tomita, *Chem. Mater.*, **12**, 3397 (2000).
8. M.-M. Titirici, M. Antonietti and N Baccile, *Green Chem.*, **10**, 1204 (2008).
9. G Buchel, K. K. Unger, A. Matsumoto and K. Tsutsumi, *Adv. Mater.*, **10**, 1036 (1998).
10. S. B. Yoon, K. Sohn, J. Y. Kim, C. H. Shin, J. S. Yu and T. Hyeon, *Adv. Mater.*, **14**, 19 (2002).
11. J. S. Yu, S. B. Yoon, Y. J. Lee and K. B. Yoon, J. *Phys. Chem. B.*, **109**, 7040 (2005).
12. F. Caruso, R. A. Caruso and H. Mohwald, *Science*, **282**, 1111 (1998).
13. J. E. Hampsey, Q. Hu, Z. Wu, J. Pang, L. Rice and Y. Lu, *Carbon*, **43**, 2977 (2005).
14. X. M. Sun and Y. D. Li, *Angew. Chem. Int. Ed.*, **43**, 597 (2004).
15. S. Iijima, *J. Cryst. Growth*, **50**, 675 (1980).
16. D. Ugarte. *Nature*, **359**, 707 (1992).
17. J. Zheng, T. C. Ekstrom, S. K. Gordeev and M. Jacob, *J. Mater. Chem.*, **10**, 1039 (2000).
18. C. He, N. Zhao, X. Du, C. Shi, J. Ding, J. Li and Y. Li, *Script. Mater.*, **54**, 689 (2006).
19. Y. Shin, G Fryxell, W. Um, K. Parker, S. V. Mattigod and R. Skaggs, *Adv. Funct. Mater.*, **17**, 2897 (2007).
20. Y. Kawabuchi, C. Sotowa, M. Kishino, S. Kawano, D. Whitehurst and I. Mochida, *Langmuir*, **13**, 2314 (1997).
21. M. Yang, M. E. Merraoui, H. Seki and K. Kaneko, *Langmuir*, **17**, 675 (2001).
22. S. Z. Yang, Y. Xia, X. Sun and R. Mokaya, *J. Phys. Chem. B.*, **110**, 18424 (2006).
23. M. M. Haley, *Chem. Mater.*, **20**, 981 (2008).
24. A. Vinu, K. Ariga, T. Mori, T. Nakanishi, S. Hishita and Y. Bando, *Adv. Mater.*, **17**, 1648 (2005).
25. W. Li, D. Chen, Z. Li, Y. Shi, Y. Wan, G Wang, Z. Jiang and D. Zhao, *Carbon*, **45**, 1757 (2007).
26. E. K. Rideal and W. M. Wright, *J. Chem. Soc.*, London, **127**, 1347 (1925).
27. W. F. Chen, F. S. Cannon and J. R. Mendez, *Carbon*, **43**, 573 (2005).
28. B. Stohr, H. P. Boehm and R. Schlogl, *Carbon*, **29**, 707 (1991).
29. V. L. Budarin, J. H. Clark, R. Luque and D. J. Macquarrie, *Chem. Commun.*, **6**, 634 (2007).
30. X. Wang, R. Liu, Z. Chen, Y. Yan, K. N. Bozhilov and P. Feng, *Chem. Mater.*, **19**, 2395 (2007).
31. M. Toda, A. Takagaki, M. Okamura, S. Hayashi, K. Domen and M. Hara *Nature*, **438**, 178 (2005).
32. Z. Li, G D. Del Cul, W. Yan, C. Liang and S. Dai, *J. Am. Chem. Soc.*, **126**, 12782 (2004).
33. L. Wang, Y. Zhao, K. Lin, X. Zhao, Z. Shan, Y. Di, Z. Sun, X. Cao, Y. Zou, D. Jiang, L. Jiang and F. S. Xiao, *Carbon*, **44**, 1336 (2006).
34. H. P. Boehm, *Carbon*, **32**, 759 (1994).
35. J. Economy, K. Foster, A. Andreopoulos and H. Jung, *Chem. Technol.*, **22**, 597 (1992).
36. C. U. Pittman, W. Jiang, G R. He and S. D. Gardner, *Carbon*, **36**, 25 (1998).
37. C. C. Hu and C. Wang, *J. Power Sources*, **125**, 299 (2004).
38. Z. Li, W. Yan and S. Dai, *Langmuir*, **21**, 11999 (2005).
39. L. R. Radovic and F. Rodriquez-Reinoso, *Chem. Phys. Carbon*, **25**, 243 (1997).
40. B. K. Pradhan and N. K. Sandle, *Carbon*, **37**, 1323 (1999).
41. P. A. Bazula, A. H. Lu, J. J. Nitz and F. Schueth, *Micropor. Mesopor. Mater.*, **108**, 266 (2008).
42. P. Vinke, M. V. Eijk, M. Verbree, A. F. Voskamp and H. Van Bekkum, *Carbon*, **32**, 675 (1994).
43. S. Jun, M. Choi, S. Ryu, H. Y. Lee and R. Ryoo, *Stud. Surf. Sci. Catal.*, **146**, 37 (2003).
44. X. Chen, M. Farber, Y. Gao, I. Kulaots, E. M. Suuberg and R. H. Hurt, *Carbon*, **41**, 1489 (2003).
45. H. Valdes, S. M. Polo, R. J. Utrilla and C. A. Zaror, *Langmuir*, **18**, 2111 (2002).
46. L. R. Radovic, I. F. Silva, J. I. Ume, J. A. Menendez, C. Leon and A. Scaroni, *Carbon*, **35**, 1339 (1997).
47. S. H. R. Abdi, Y. J. Kim, Y.-K. Park and C. W. Lee, *Chem. Lett.*, **36**, 1202 (2007).
48. B. Fang and L. Binder, *J. Phys. Chem. B.*, **110**, 7877 (2006).
49. K. H. Vase, A. H. Holm, K. Norrman, S. U. Pedersen and K. Daasbjerg, *Langmuir*, **23**, 3786 (2007).
50. M. Delamar, R. Hitmi, J. Pinson and J. M. Saveant, *J. Am. Chem. Soc.*, **114**, 5883 (1992).
51. X. Wang, D. E. Jiang and S. Dai, *Chem. Mater.*, **20**, 4800 (2008).
52. D. Yu, Z. Wang, N. S. Ergang and A. Stein, *Stud. Surf. Sci. Catal.*, **165**, 365 (2007).
53. R. E. Botto and Y. Sanada, *Adv. Chem. Series*, **229**, ACS, Washington DC (1993).
54. C. J. Meyers, S. D. Shah and S. C. Patel, *J. Phys. Chem. B.*, **105**, 2143 (2001).
55. C. G Bac, P. Bernier and S. Latil, *Curr. Appl. Phys.*, **1**, 149 (2001).
56. A. J. G Zarbin, R. Bertholdo and M. A. F. C. Oliveira, *Carbon*, **40**, 2413 (2002).
57. H. Muller, P. Rehak, C. Jager, J. Hartmann, N. Meyer and S. Spange, *Adv. Mater.*, **12**, 1671 (2000).
58. J. Z. Hu, M. S. Solum, C. M. V. Taylor, R. J. Pugmire and D. M. Grant, *Energy & Fuels*, **15**, 14 (2001).
59. Y. Adachi and M. Nakamizo, *Adv. Chem. Ser.*, **229**, 269 (1993).
60. F. Leroux and M. Dubois, *J. Mater. Chem.*, **16**, 4510 (2006).
61. G E. Maciel, C. E. Bronnimann and C. F. Ridenour, *Adv. Chem. Ser.*, **229**, 27 (1993).
62. J. Zawadzki, *Chem. Phys. Carbon*, **21**, 147 (1989).
63. J. Zawadzki, P. A. Thrower and M. Dekker, C*hem. & Phys. Carbon*, **21**, 147 (1988).

64. P. Painter, M. Starsinic and M. Coleman, *Fourier Transform Infrared Spectrosc*., **4**, 169 (1985).
65. M. C. Blanco Lopez, M. Alonso and J. M. D. Tascon, *Micropor. Mesopor. Mater.*, **34**, 171 (2000).
66. X. Quan, X. T. Liu, L. L. Bo, S. Chen, Y. Z. Zhao and X. Y. Cui, *Water Res.*, **38**, 4484 (2004).
67. J. Przepiorski, M. Skrodzewicz and A. W. Morawski, *Appl. Surf. Sci.*, **225**, 235 (2004).
68. R. Escribano, J. J. Sloan, N. Siddique and N. Dudev, *Vibrational Spectroscopy*, **26**, 179 (2001).
69. N. Shimodaira and A. Masui, *J. Appl. Phys.*, **92**, 902 (2002).
70. R. J. Nemanich and S. A. Solin, *Phys. Rev. B.*, **20**, 392 (1979).
71. Y. Wang, D. C. Alsmeyer and R. L. McCreery, *Chem. Mater.*, **2**, 557 (1990).
72. D. G. McCulloch, S. Prawer and A. Hoffman, *Phys. Rev. B.*, **50**, 5905 (1994).
73. D. Y. Qu and H. Shi, *J. Power Sources*, **74**, 99 (1998).
74. P. Andrew and M. A. P. Sherwood, *Carbon*, **21**, 53 (1983).
75. P. E. Vickers, J. F. Watts, P. Christian and M. C. Mohamed, *Carbon*, **38**, 675 (2000).
76. U. Zielke, K. J. Huttinger and W. P. Hoffman, *Carbon*, **34**, 983 (1996).
77. J. L. Figueiredo, M. F. R. Pereira, M. M. A. Freitas and J. J. M. Orfao, *Carbon*, **37**, 1379 (1999).
78. H. Darmstadt, C. Roy, S. Kaliaguine, S. J. Choi and R. Ryoo, *Carbon*, **40**, 2673 (2002).
79. Y. Otake and R. G. Jenkins, *Carbon*, **31**, 109 (1993).
80. B. Xiao, J. P. Boudou and K. M. Thomas, *Langmuir*, **21**, 3400 (2005).
81. H. P. Boehm, *Carbon*, **40**, 145 (2002).
82. E. Papirer, J. Dentzer, S. Li and J. B. Donnet, *Carbon*, **29**, 69 (1991).
83. H. Tamon and M. Okazaki, *Carbon*, **34**, 741 (1996).
84. E. Papier, S. Li and J. Donnet, *Carbon*, **25**, 243 (1987).
85. D. S. Cameron, S. J. Cooper, I. L. Dodgson, B. Harrison and J. W. Jenkins, *Catal. Today*, **7**, 113 (1990).
86. H. P. Boehm, *High Temp-High Pressures*, **22**, 275 (1990).
87. H. W. Hillhouse, J. W. van Egmond, M. Tsapatsis, J. C. Hanson and J. Z. Larese, *Micropor. Mesopor. Mater.*, **44-45**, 639 (2001).
88. E. Smorgonskaya, R. Kyutt, A. Danishevskii, C. Jardin, R. Meaudre, O. Marty, S. Gordeev and A. Grechinskaya, *J. Non-Crystalline Solids*, **299-302**, 810 (2002).
89. Y. Venhryn, I. I. Grygorchak, Yu. O. Kulyk, S. I. Mudry and R. Shvets, *Optica Applicata*, **38**, 119 (2008).
90. M. H. Lim, C. F. Blanford and A. Stein, *Chem. Mater.*, **10**, 467 (1998).
91. Y. Wang, D. Nepal and K. E. Geckeler, *J. Mater. Chem.*, **15**, 1049 (2005).
92. F. Rouquerol, J. Rouquerol and K. Sing, Adsorption by Powders & Porous Solids, Academic, San Diego, CA (1999).
93. M. R. Bhambhani, P. A. Cutting, K. S. W. Sing and D. H. Turk, *J. Colloid Interf. Sci*., **38**, 109 (1972).
94. J. Kenneth and B. McEnaney, *J. Colloid Interf. Sci*., **95**, 340 (1983).
95. J. Choma, J. Gorka and M. Jaroniec, *Micropor. Mesopor. Mater.*, **112**, 573 (2008).
96. P. I. Ravikovitch and A. V. Neimark, *Langmuir*, **18**, 1550 (2002).
97. J. J. Lee, S. Han, H. Kim, J. H. Koh, T. Hyeon and S. H. Moon, *Catal. Today*, **86**, 141 (2003).
98. J. H. Zhou, J. P. He, Y. J. Ji, W. J. Dang, X. L. Liu, G. W. Zhao, C. X. Zhang, J. S. Zhao, Q. B. Fu and H. P. Hu, *Electrochim. Acta*, **52**, 4691 (2007).
99. K. I. Min, J. S. Choi, Y. M. Chung, W. S. Ahn, R. Ryoo and P. K. Lim, *Appl. Catal. A*, **337**, 97 (2008).
100. T. Harada, S. Ikeda, M. Miyazaki, T. Sakata, H. Mori and M. Matsumura, *J. Mol. Catal. A*, **268**, 59 (2007).
101. E. Sipos, G. Fogassy, A. Tungler, P. V. Samant and J. L. Figueiredo, *J. Mol. Catal. A*, **212**, 245 (2004).
102. M. Hara, T. Yoshida, A. Takagaki, T. Takata, J. N. Kondo, S. Hayashi and K. Domen, *Angew. Chem. Int. Ed*., **43**, 2955 (2004).
103. Y. Idota, T. Kubota, A. Matsufuji, Y. Maekawa and T. Miyasaka, *Science*, **276**, 1395 (1997).
104. M. Noh, Y. Kwon, H. Lee, J. Cho, Y. Kim and M. G. Kim, *Chem. Mater.*, **17**, 1926 (2005).
105. S. H. Ng, J. Wang, D. Wexler, S. Y. Chew and H. K. Liu, *J. Phys. Chem. C*, **111**, 11131 (2007).
106. R. D. Cakan, M. M. Titirici, M. Antonietti, J. Maier and Y. S. Hu, *Chem. Commun.*, 3759 (2008).
107. J. M. Tarascon and M. Armand, *Nature*, **414**, 359 (2001).
108. S. J. Han, B. C. Jang, T. Kim, S. M. Oh and T. Hyeon, *Adv. Funct. Mater.*, **15**, 1845 (2005).
109. Y. Wang, F. Su, J. Y. Lee and X. S. Zhao, *Chem. Mater.*, **18**, 1347 (2006).
110. J. Fan, T. Wang, C. Yu, B. Tu, Z. Jiang and D. Zhao, *Adv. Mater.*, **16**, 1432 (2004).
111. N. S. Ergang, J. C. Lytle, K. T. Lee, S. M. Oh, W. H. Smyrl and A. Stein, *Adv. Mater.*, **18**, 1750 (2006).
112. Q. Pan, H. Wang and Y. Jiang, *J. Mater. Chem.*, **17**, 329 (2007).
113. E. Frackowiak and F. Beguin, *Carbon*, **39**, 937 (2001).
114. J. Hong, I. H. Yeo and W. Paik, *J. Electrochem. Soc.*, **148**, 156, (2001).
115. C. C. Hu and T. W. Tsou, *J. Power Sources*, **135**, 179 (2003).
116. M. Winter and R. J. Brodd, *Chem. Rev.*, **104**, 4245 (2004).
117. B. L. Groenendaal, F. Jonas, D. Freitag, H. Pielartzik and J. R. Reynolds, *Adv. Mater.*, **12**, 481 (2000).
118. H. Li, H. A. Xi, S. Zhu, Z. Wen and R. Wang, *Micropor. Mesopor. Mater.*, **96**, 357 (2006).